*Energy Equip. Sys./ Vol. 7/No. 1/March 2019/* 1-10

ENERGY EQUIPSYS

**Energy Equipment and Systems**

http://energyequipsys.ut.ac.ir
www.energyequipsys.com

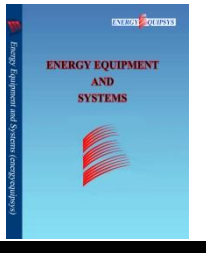


# Numerical simulation of incompressible turbulent flow in shrouded disk system with radial outflow

**Author**

**Milad Charmchi** [a]
**Saadat Zirak** [a*]

[a] Mechanical Engineering Department, Semnan University, Semnan, Iran

**ABSTRACT**

*The flow behavior inside the shrouded disk system is of importance in appropriate design of turbomachinery cavities and turbine test cell hydraulics dynamometer .The turbulent incompressible flow is analyzed for the shrouded disk system with axial clearance. The flow core behaves as a Batchelor type structure when a weak inflow is imposed on the disk cavity. By increasing the inflow, the central core disappears and the tangential velocity distribution is changed to Stewartson type structure. The central core again reappears by increasing the Reynolds number. The moment coefficient of rotary disk depends on superimposed flow rate coefficient and dimensionless geometrical parameters. Moment coefficient increases with increasing inflow rate while the other parameters remain constant. The coefficient is reduced by increasing the Reynolds number. Moreover, it increases with both increasing rotary and stationary disks axial distance, and decreasing clearance ratio. The experimental results of a cavity with radial clearance are used to validate the accuracy of the simulation. The results of this analysis and its development can be used in the design of turbine test cell hydraulics dynamometers.*

*Article history*:

Received : 6 January 2018
Accepted : 6 October 2018

**Keywords:** Rotary & Stationary Disk, Batchelor & Stewartson Flow, Incompressible, Cavity Flow, Dynamometer, Moment Coefficient.

## 1. Introduction

Flow analysis inside the cavities is a basic step in the design of both turbine test cell hydraulics dynamometer (incompressible) and cavity design created from gas turbines rotor/stator interfaces (compressible). The hydraulics dynamometer can be faced with unwanted cavitation in the low-pressure regions of around the rotation axis. The compressible counterparts of cavity flows are the flow of secondary air system cooling stream between the stator and rotor disks of axial turbines. In the later, an improper cavity design may affectboth the performance features and shaft resonance parameters.

The cavity flow also is experienced in various locations of turbomachines. In Fig. 1, positions 6, 7 and 8 shows the shrouded type spaces for cavity flows. Daily and Nece (1960) investigated the compressible air flow inside an enclosed rotating cavity experimentally and numerically. They studied the effect of both rotational speed and cavity gap size variations on fluid pressure, flow angular speed and rotor moment. They observed four flow regimes inside the cavity depend on tangential Reynolds number and the gap size between the rotating and stationary disks. Those are:

i) Laminar regimes with non-mixed rotor and stator boundary layers, $G<0.03$ and $Re_\theta<10$

[*] Corresponding author: Saadat Zirak
Mechanical Engineering Department, Semnan University, Semnan, Iran
Email: s_zirak@semnan.ac.ir

ii) Laminar regimes with mixed rotor and stator boundary layers
iii) Turbulent regimes with non-mixed rotor and stator boundary layers
iv) Turbulent regimes with mixed rotor and stator boundary layers

Recently, Hu et al. (2017) refers to above four flow regimes and describes the common centripetal through-flow from the outer radius of the impeller to the impeller eye in centrifugal pumps and turbines. They thought it has a strong effect on radial pressure distribution, axial thrust, and frictional torque. In this research, the influence of changing circumferential Reynolds number and dimensionless axial gap width on flow parameters is investigated. Also, the 2-D analyzes of previous works are developed to a 3-D one by introducing the through-flow coefficient.

In literature, there are not much research on cavities with the superimposed flow. The imposed flow may affect the flow behavior inside the cavity considerably by changing the boundary layer thicknesses on rotor and stator and hence flow regime. Kurokawa and Sakuma (1988) mentioned the boundary layers interference and transition from laminar to turbulent due to the imposed flow.

Bayley and Owen (1969) analyzed the compressible air flow inside the cavity of rotating and stationary walls and investigated the effect of imposed inflow in the case of radial clearance outlet to the atmosphere and clearance sizes of G=0.008 and 0.03. They used the finite difference method to solve the boundary layer equations. They considered non swirled imposed turbulent flow with $\mathrm{Re}_\theta = 3 \times 10^5$. The obtained results showed an increase of disk moment with increasing imposed flow rate because the core rotation is lowered.

Altmann (1972) solved the compressible flow cavity with clearances of G=0.056 and 0.15. It mentioned the negligible effect of disks distance on core rotation and disk moment. Moreover, it showed that the frictional resistance of the rotating disk is considerably lowered for increased core rotation values.

Iacovides and Toumpanakis (1993) solved the compressible axisymmetric Navier-Stokes equations in a closed cavity. They applied four various turbulent models. Those were: one equation coupled k-ε, Sharma and Launder k-ε, k-ω, and a low Reynolds stress differential equation model. The k-ε and k-ω predicted the laminar boundary layer with good accuracy but the Reynolds stress model was not reasonable.

Haddadi and Poncet (2008) investigated incompressible flow with low Reynolds model for cavities of small gaps. They showed that the previously mentioned four regimes of Daily and Nece are applicable for cavities with imposed inflow. Moreover, they limited the turbulence effects to boundary layers and neglected Reynolds stress components in the cavity core flow.

The previous incompressible studies were limited to cavities with radial clearance outlet. The idea of studying the axial clearance almost started from the works of Bayley and Owen (1970), and Phadke and Owen (1983). The cavities are shrouded, and the outflow passes through an axial clearance outlet. They investigated the pressure distribution inside the cavities for various rotating disk angular velocities. Also, they investigated the effects of geometry variations, Reynolds number, and imposed inflow mass flow rate on disk moment.

In the present work, the incompressible turbulent flow of shrouded cavity with an axial clearance is analyzed. The cavity gap is large and the flow regime is placed in domain iv.
In a new study, Launder et al. (2010) reviewed comprehensively the range of flow inside the annular cavities in which one of the disks is rotating, and the other is stationary. They confined the research to the case where the disk spacing is small compared to disk radius; it implies no through-flow. At low Reynolds numbers, an axisymmetric flow is observed with radially outward near the moving wall and returning along the stationary one. As the Reynolds number is raised, it changes to a shear flow with vortices near both disks. At higher Reynolds numbers, a complex organized structure is dominant in the turbulent regime. This last behavior, in the 20th Century both experimental and computational studies treated as axisymmetric and steady.

## Nomenclature

| | |
|---|---|
| $b$ | rotating disk radius |
| $C_m$ | moment coefficient |
| $C_p$ | pressure coefficient |
| $C_w$ | Imposed flow coefficient |
| $I_1$ | axial clearance |
| $I_3$ | radial clearance |
| $G = \frac{s}{b}$ | gap ratio |

| | |
|---|---|
| $G_a = \frac{I_1}{b}$ | axial distance ratio |
| $G_r = \frac{I_3}{b}$ | radial distance ratio |
| $M = \int_0^b \tau_{z\theta}\, r(2\pi r dr)$ | rotating disk moment |
| $p^* = \frac{p}{1/2\,\rho\Omega^2 b^2}$ | pressure ratio |
| $Re_\theta = \frac{\Omega b^2}{\vartheta}$ | rotational Reynolds number |
| $R$ | radial distance from disc centerline |
| $r^* = \frac{r}{b}$ | radius ratio |
| $s$ | axial clearance between shrouded stator and rotor |
| $v_r$ | radial velocity |
| $v_\theta$ | tangential velocity |
| $\mathrm{v}_\mathrm{r}^*$ | radial velocity ratio |
| $\mathrm{v}_\theta^*$ | tangential velocity ratio |
| Z | axial distance from rotating disk |
| $\mathrm{z}^* = \frac{\mathrm{z}}{\mathrm{s}}$ | axial distance ratio |
| $\rho$ | density |
| $\tau_{z\theta}$ | shear stress |
| $\vartheta$ | kinematic viscosity |
| $\Omega$ | disc angular velocity |

**Superscripts**

| | |
|---|---|
| $*$ | dimensionless |

***Subscripts***

| | |
|---|---|
| $a$ | axial |
| $r$ | radial |
| $\theta$ | tangential |

## 2. Geometry and parameters

Figures 2 and 3 show the physical domain of the cavity with axial and radial outlet gaps, respectively. The stator is shrouded and the rotor is rotating with an angular velocity of Ω. The dimensionless axial distance of the two disks varies from G = 0.012 to 0.048. The dimensionless gap size, radially and axially ($G_r$ and $G_a$), is in a range of 0.006 to 0.012.

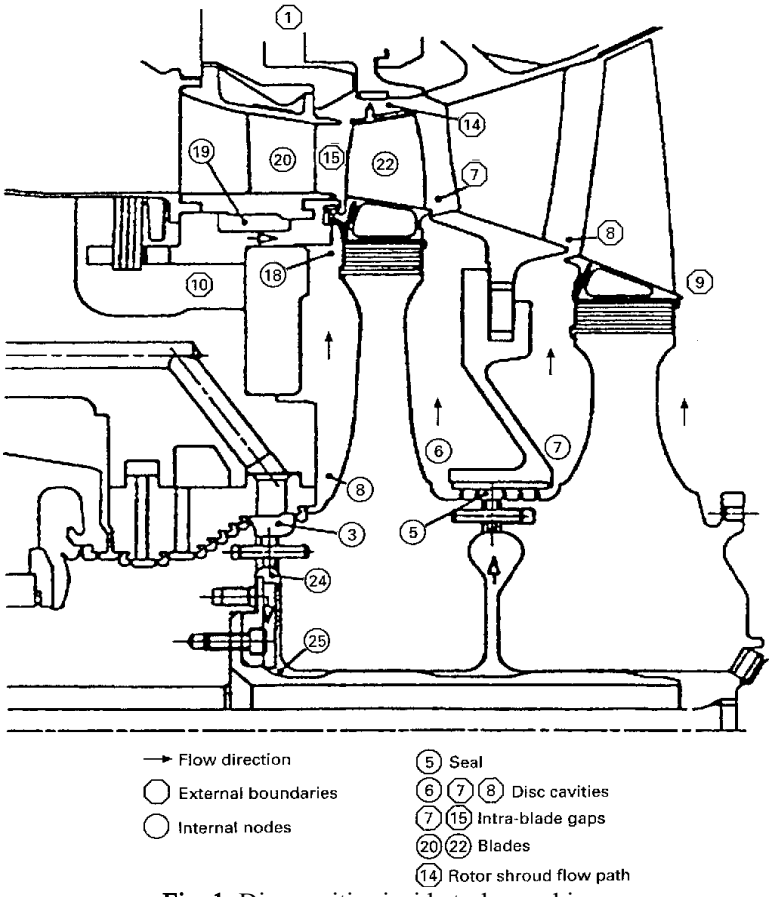


**Fig. 1.** Disc cavities inside turbomachines

The imposed flow enters from the central eye region of the stator and exits through the gaps. In this respect, the main flow configuration is outward, i.e. to the outer radius, which is called centrifugal, unlike the case of centripetal which the flow enters through the gaps and exists from the central regions of the stator.

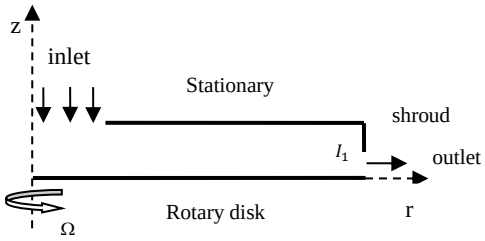


**Fig. 2.** Disk system with axial clearance

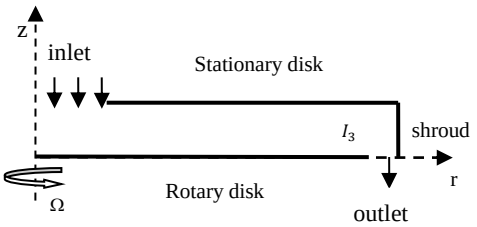


**Fig. 3 .**Disk system with radial clearance

By considering the moment inserted on the rotating disk, the moment coefficient is defined as;

$$C_m = \frac{M}{0.5\rho\Omega^2 b^5} \tag{1}$$

The flow coefficient is expressed based on the imposed flow rate;

$$C_w = \frac{Q}{\vartheta b} \tag{2}$$

Pressure coefficient, which is a determinant factor for the cavity flows, can be defined as below:

$$C_p = p^*(r^*) - p^*(0.92) \tag{3}$$

where the $p^*$ is dimensionless pressure.

Poncet et al. (2005), suggested considering the pressure at $r^* = 0.92$ as a reference value.

Radial and axial dimensionless velocities are;

$$v_r^* = \frac{v_r}{r\Omega} \tag{4}$$

$$v_\theta^* = \frac{v_\theta}{r\Omega}$$

## 3.Governing equations

The steady incompressible continuity and momentum equations govern the cavity flow. The turbulent appears in terms of Reynolds stresses.

$$\frac{\partial(u_i)}{\partial x_i} = 0 \tag{5}$$

$$\rho\frac{\partial}{\partial x_j}(u_i u_j) = -\frac{\partial p}{\partial x_j} + \frac{\partial}{\partial x_j}\left[\mu\left(\frac{\partial u_i}{\partial x_j} + \frac{\partial u_j}{\partial x_i} - \frac{2}{3}\delta_{ij}\right)\right] + \frac{\partial}{\partial x_j}\left(-\rho\overline{u_i' u_j'}\right) \tag{6}$$

In which, $\delta_{ij}$ is the Kronecker Delta.

By using the Boussinesq assumption, the Reynolds stress terms can be expressed as;

$$-\rho\overline{u_i' u_j'} = 2\mu_t S_{ij} - \frac{2}{3}(\rho k)\delta_{ij} \tag{7}$$

where, $S_{ij}$ is the mean strain rate tensor and relates to velocity gradients by;

$$S_{ij} = \frac{u_{i,j} + u_{j,i}}{2} \tag{8}$$

## 4. RNG K- $\varepsilon$ turbulence model

Orszag et al. (1993) suggested the RNG k-ε model as an improvement of standard k-ε for rapidly strained flows and swirl flows. Also, the model better acts in small Reynolds number near the walls. The RNG k-ε turbulent kinetic energy and dissipation rate equations are,

$$\rho\frac{\partial}{\partial x_i}(k u_i) = \frac{\partial}{\partial x_j}\left(\alpha_k \mu_{eff}\frac{\partial k}{\partial x_j}\right) + G_k + G_b - \rho\varepsilon - Y_M + S_K \tag{9}$$

$$\rho\frac{\partial}{\partial x_i}(\varepsilon u_i) = \frac{\partial}{\partial x_j}\left(\alpha_\varepsilon \mu_{eff}\frac{\partial \varepsilon}{\partial x_j}\right) + C_{1\varepsilon}\frac{\varepsilon}{k}(G_k + C_{3\varepsilon}G_b) - C_{2\varepsilon}\rho\frac{\varepsilon^2}{k} - R_\varepsilon + S_\varepsilon \tag{10}$$

The main difference between the RNG k- $\varepsilon$ and the standard k- $\varepsilon$ is the additional term of $R_\varepsilon$ in the $\varepsilon$ equation given by,

$$R_\varepsilon = \frac{C_\mu \rho \eta^3 \left(1 - {}^{\eta}/_{\eta_0}\right)}{1 + \beta \eta^3} \frac{\varepsilon^2}{k} \quad (11)$$

where, $\eta = S\, {}^{K}/_{\varepsilon}$ and

$$S = \sqrt{2 S_{ij} S_{ij}} = \sqrt{{}^{G}/_{\mu_t}} \quad (12)$$

In previous relations, the turbulent viscosity is;

$$\mu_t = \rho C_\mu \frac{k^2}{\varepsilon} \quad (13)$$

## 5.Method of solution

The incompressible flow inside the cavity of rotating and stationary disks is solved using the ANSYS FLUENT solver. The pressure-based algorithm is used, and the axisymmetric rectangular physical domain is analyzed. The mass flow inlet and pressure outlet are considered as boundary conditions. The turbulence intensity of 1% at the inlet and 5% at the outlet is applied. The corresponding hydraulic diameter is 0.11 and 0.006 m, respectively. The rotor wall is rotating and the no-slip condition is applied to the shrouded stator. The meshing is performed in ANSYS WORKBENCH. The selected mesh maintains the y+ values about unity on the walls. Figure 4 shows a segment of the meshed domain. The PRESTO method is applied to pressure equation and for others, the second order UPWIND is used. The convergence is accepted for the residuals less than $10^{-7}$. The working fluid is water, and its properties are given in Table 1.

## 6.Assessment of method

To evaluate the method, the numerical results of a cavity with radial clearance are compared with experimental and numerical results of Poncet et al. (2005). They applied the Shear Stress Transport (SST) turbulence model in their numerical works. In the present work, which the results of the pressure coefficient are shown in Figs. 5 to 7, the maximum value of y+ on rotating and stationary walls is about unity. The results are given at $\mathrm{Re}_\theta = 4.15 \times 10^6$, and for various flow coefficients of $C_w$= -1976, -5929, and, -9881 (centripetal throughflow). For the regions away from the center of rotation, the results are in good agreement with the experimental values. Around the cavity axis, some discrepancy is observed which can be due to the difference between the experimental setup and the simulation geometry. Grid independence is checked by investigating three different mesh densities on the predictions of pressure coefficient value shown in Table 2. For the last two grid sizes, the difference in $C_p$ is about 1.1%.

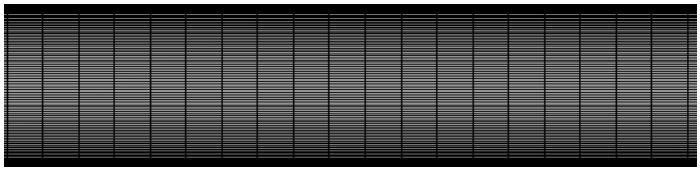

**Fig. 4 .**A segment of the meshed domain

**Table 1.** Water properties

| Property | Unit | Value |
|---|---|---|
| Kinematic viscosity | $m^2.s^{-1}$ | $10^{-6}$ |
| Density | $kg.m^{-3}$ | 1000 |

**Table 2.** Pressure coefficient changes with the cell number for $\mathrm{Re}_\theta = 4.15 \times 10^6$, and $C_w = -5929$ in $r^* = 0.56$

| Mesh | Cell number | $C_P$ | changes |
|---|---|---|---|
| Mesh #1 | 15300 | -0.061 | - |
| Mesh #2 (main mesh) | 25300 | -0.0578 | 5.3% |
| Mesh #3 | 50600 | -0.057 | 1.4% |

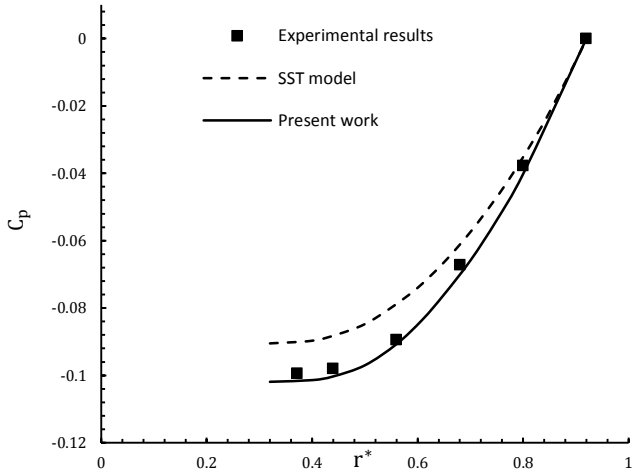


**Fig. 5** .Radial pressure distribution for $\mathrm{Re}_\theta = 4.15 \times 10^6$ , $\mathrm{C_w} = -1976$

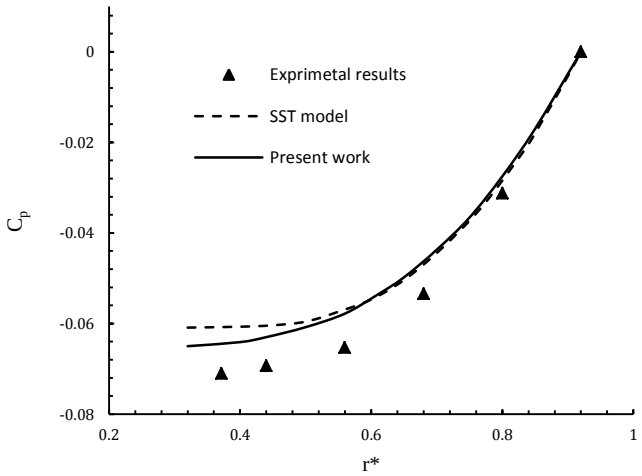


**Fig .6.** Radial pressure distribution for $\mathrm{Re}_\theta = 4.15 \times 10^6$ , $\mathrm{C_w} = -5929$

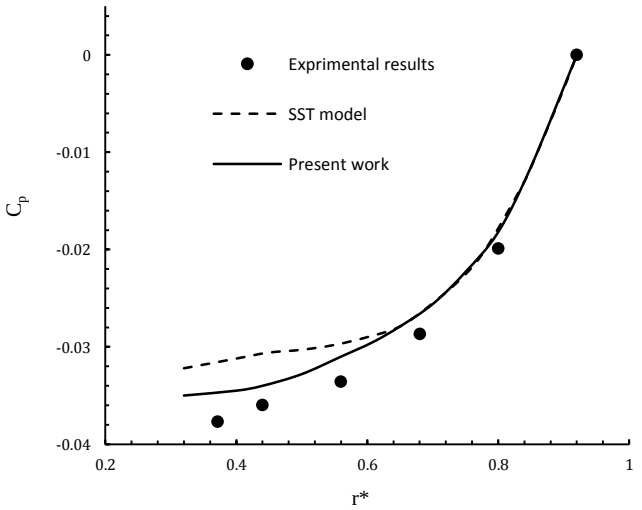


**Fig. 7.** Radial pressure distribution for $\mathrm{Re}_\theta = 4.15 \times 10^6$ , $\mathrm{C_w} = -9881$

## 7. Results

### 7.1. Pressure coefficient and velocity components profiles

The results of the shrouded disk system with axial clearance (radial outflow) are presented for the water as the working fluid. Selected dimensionless radii are 0.44, 0.56, and, 0.80. The results are given for Reynolds numbers from 10^5 to 10^7 at imposed flow coefficients of -1976, -5929, and -9881. In all the cases, the checked y+ on the walls is not much above unity.

The pressure coefficient is determined from Eq. (3). Figure 8 shows the radial pressure coefficient distribution for various flow coefficients at $\mathrm{Re}_\theta = 4.15 \times 10^6$. As it is expected, the pressure coefficient decreases toward the cavity central region; always showing a negative value for $C_p$. Moreover, in a given radius, increasing the imposed centripetal flow increases the pressure coefficient. In other words, the imposed centripetal throughflow causes a more uniform pressure in the cavity. In the case with $C_w = -5929$, radial variation of pressure is negligible for r<0.55. This shows a Stewartson flow structure while that is changed to a Batchelor structure for r>0.55.

Dimensionless tangential and radial velocity components, between the two disks for the centripetal flow of $C_w = -5929$, are compared in Figs. 9 and 10, respectively, at various radial positions. As it is observed, the two wall boundary layers are separated by a central rotating core at r*=0.8, while the core is going to be diminished in the inner regions of the disks. The radial component of velocity, at r*=0.8, is outward on rotating disk (Ekman layer) and it behaves inward on stationary disk (Bodewadt layer). Around the mid and inner radial regions, it shows an outward flow in all axial positions.

The effect of changing Reynolds number on velocity components is observed in Figs. 11 and 12 at r*=0.56. By increasing the Reynolds number, the radial component of flow velocity inside the stator boundary layer is directed centripetal, and the flow core again reappears. In a given Reynolds number, the flow structure is changed from Batchelor to a Stewartson type with closing to the central regions. The variations are negligible for high Reynolds number. The analysis shows structure change from Batchelor to Stewartson in the following cases;

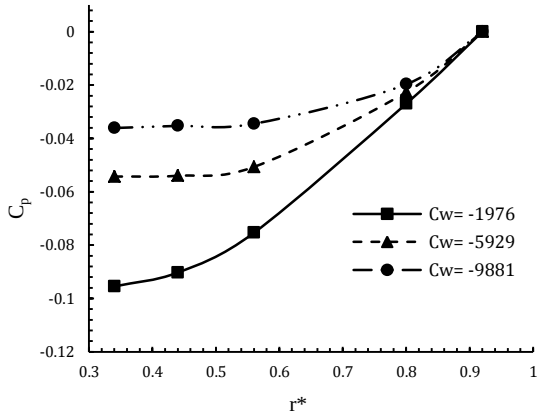


**Fig. 8.** Radial pressure coefficient distribution for $\mathrm{Re}_\theta = 4.15 \times 10^6$, G=0.036 and three centrifugal throughflow

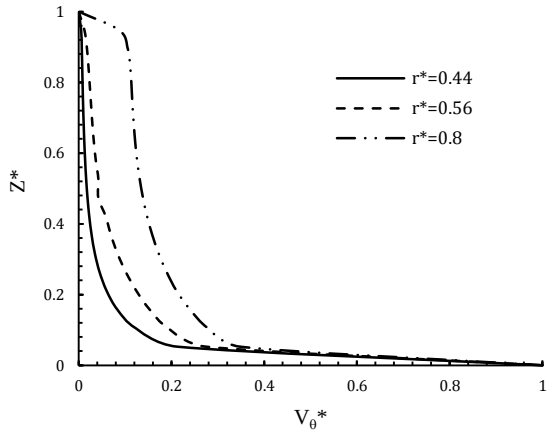


**Fig. 9.** Mean tangential velocity profile for $C_w = -5929$, G=0.036, $\mathrm{Re}_\theta = 10^6$ at three radial locations r*

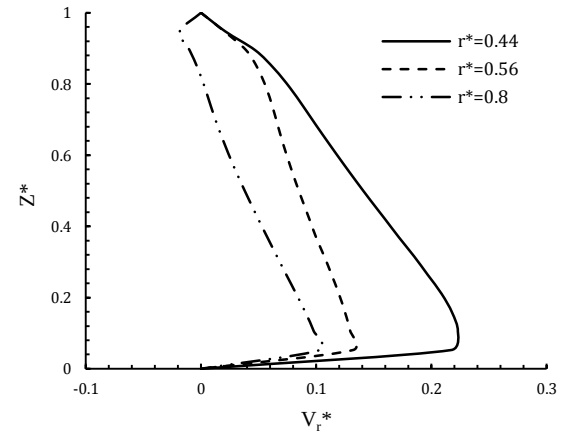


**Fig. 10.** Mean radial velocity profile for $C_w = -5929$, G=0.036, $\mathrm{Re}_\theta = 10^6$ at three radial locations r*

1- With closing to central regions,
2- With increasing of imposed flow rate,
3- With decreasing the Reynolds number.

This structure change mainly depends on the radial component of velocity. In Stewartson structure, the radial component is outward (positive) for all axial positions, while that is almost zero in Batchelor type.

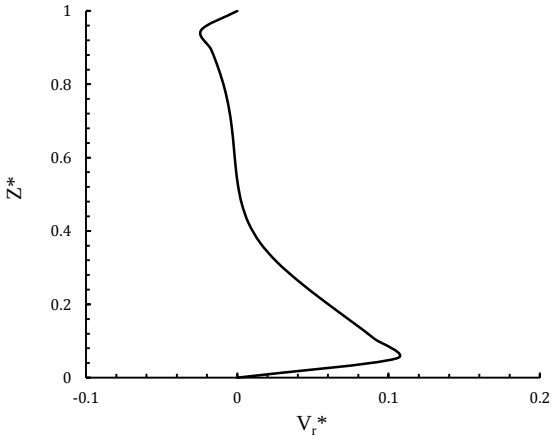


**Fig. 11**. Axial profile of mean radial velocity for $\mathrm{Re}_\theta = 4.15 \times 10^6$ and $\mathrm{C_w} = -5929$

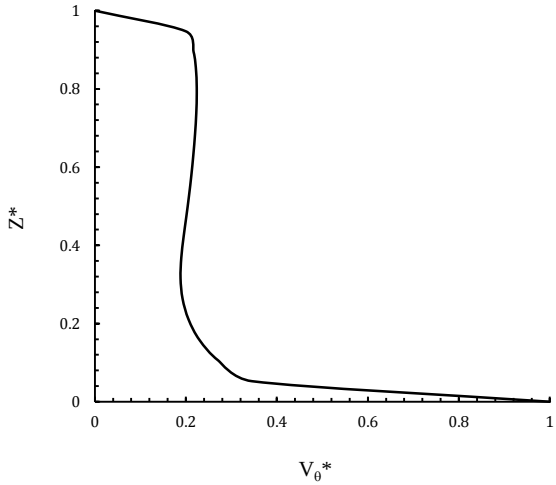


**Fig. 12.** Axial profile of mean tangential velocity for $\mathrm{Re}_\theta = 4.15 \times 10^6$ and $\mathrm{C_w} = -5929$

## 7.2 Moment coefficient of rotating disk

Rotating disk moment is one of the most important parameters of the rotor-stator cavity system. In this section, the effect of axial and radial clearance ratio, Reynolds number and impose flow rate on moment coefficient of the rotary disk with radial and axial inflow are checked. Moment coefficient of the rotary disk is calculated in accordance with Eq.(1). Figures 13 and 14 show the effect of imposed inflow on moment coefficient. The results are given for Reynolds numbers from $10^5$ to $10^7$ at mass flow coefficients of -1976, -5929, and -9881. As it is observed, moment coefficient is increased with increasing mass flow of imposed inflow. Figures 15 and 16 show the effect of gap size on moment coefficient, which increases with increasing the gap ratio. The effect of axial and radial distance ratio on moment coefficient can be observed in Figs. 17 and 18. By increasing the radial and axial distance ratio, the moment coefficient is decreased.

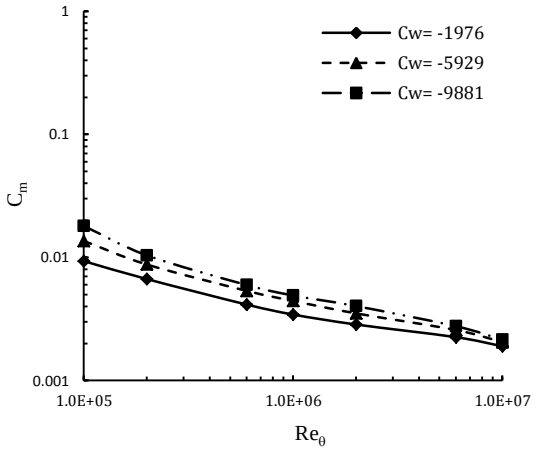


**Fig. 13.** Effect of flow rate coefficient on moment coefficient in cavity with axial clearance for $\mathrm{G} = 0.012$ and $\mathrm{G_a} = 0.012$

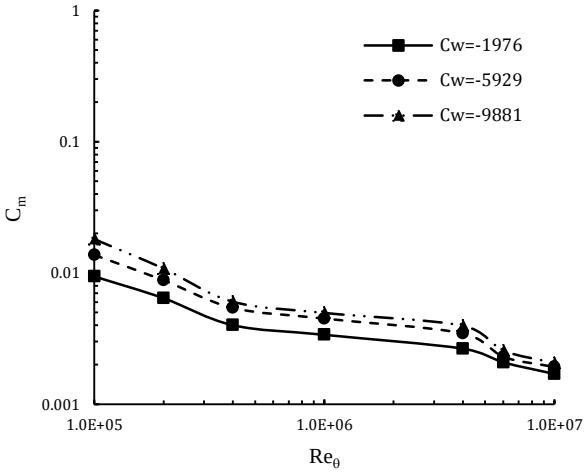


**Fig. 14.** Effect of flow rate coefficient on moment coefficient in the cavity with radial clearance for $\mathrm{G} = 0.012$ and $\mathrm{G_r} = 0.012$

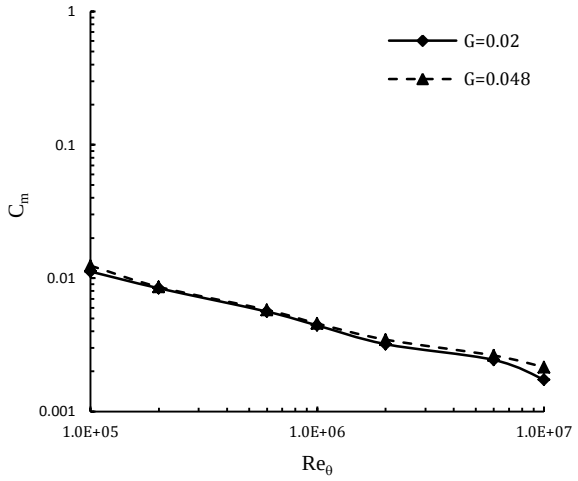


**Fig. 15.** Effect of gap width ratio on moment coefficient in the cavity with axial clearance for $G_a = 0.012$ and $C_w = -5929$

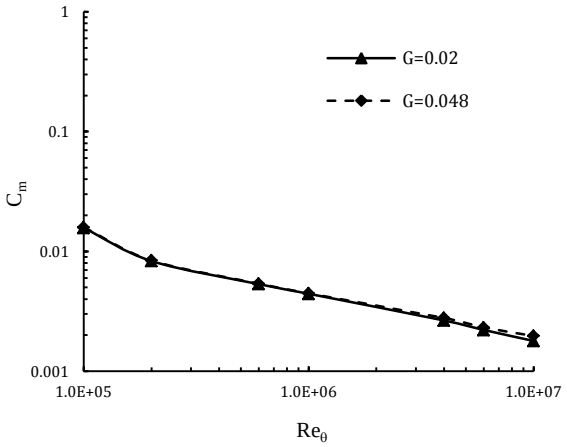


**Fig. 16.** Effect of gap width ratio on moment coefficient in the cavity with radial clearance for $G_r = 0.012$ and $C_w = -5929$

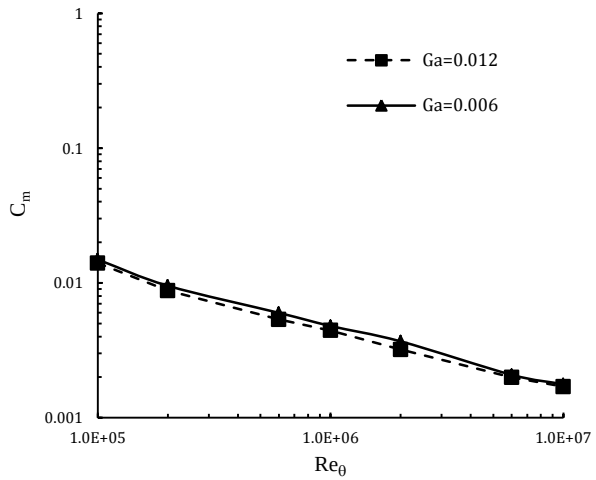


**Fig. 17.** Effect of axial distance ratio on moment coefficient in the cavity with axial clearance for $G = 0.012$ and $C_w = -5929$

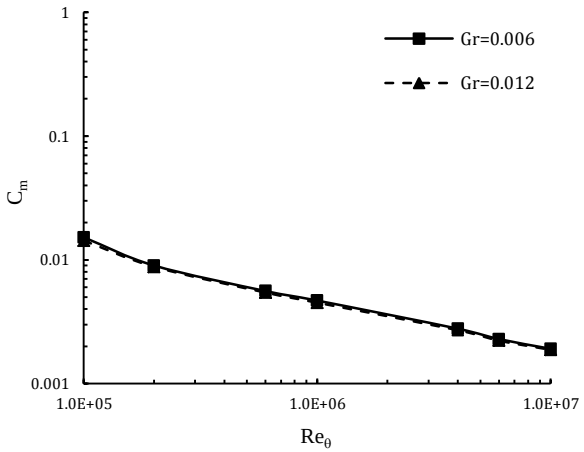


**Fig. 18.** Effect of radial distance ratio on moment coefficient in the cavity with radial clearance for $G = 0.012$ and $C_w = -5929$

## 8.Conclusion

In this study, the turbulent incompressible flow of water in a shrouded disk system with radial outflow is analyzed. This geometry can be utilized in the design of turbine cell hydrodynamic dynamometer. An axisymmetric numerical solution is used to analyze the flow. Experimental and numerical results of the cavity with axial outflow is used to validate the performed numerical method and selected turbulence model. Acceptable accuracy was observed comparing RNG k-ε turbulent model results with experiment. The flow structure is bachelor type with non-mixed rotor and stator boundary layers together with rotary core for weak superimposed flow rate. Rotating core gradually disappears with increasing the imposed flow rate, and flow structure becomes Stewartson type. In this case, the tangential velocity of flow is negligible and the radial velocity is positive everywhere in the cavity. Moreover, moment coefficient of rotating disk shows an increasing trend. By increasing the Reynolds number, the radial component of flow velocity inside the stator boundary layer is directed centripetal and the flow core again reappears. Moment coefficient of rotating disk increases with increasing clearance between shrouded stator and rotor and decreases with increasing axial clearance.

## References

[1] Daily J.W., Nece R.E., Chamber Dimension Effects on Induced Flow and Frictional Resistance of Enclosed Rotating

Disk", Journal of Basic Engineering 82: 217-232(1960).
[2] Hu B., Brillert D., Dohmen H. J., Karl Benra F., Investigation on the Flow in a Rotor-Stator Cavity with Centripetal Through-Flow, International Journal of Turbomachinery, Propulsion and Power (2017).
[3] Kurokawa J., Sakuma M,, Flow in a Narrow gap along an Enclosed Rotating Disk with Through-Flow", JSME International Journal, Series II, 31(2): 243-25 (1988).
[4] Bayley F.J., Owen J.M., Flow between a Rotating and a Stationary Disc, Aeronautical Quarterly, 20: 333-354 (1969).
[5] Altmann D., Beitrag Zur Berechnung Der Turbulenten Strömung im Axialspalt Zwischen Laufrad und Gehäuse von Radialpumpen, Dissertation, TU Magdeburg (1972).
[6] Iacovides H., Toumpanakis, Turbulence Modeling of Flow in Axisymmetric Rotor-Stator Systems, 5th International Symposium on Refined Flow Modelling and Turbulence Measurements, Paris, The International Association for Hydro-Environment Engineering and Research, 835-842 (1993).
[7] Haddadi S., Poncet S., Turbulence Modeling of Torsional Couette Flows, International Journal of Rotating Machinery, 2008: 2008, Article ID 635138, 27.
[8] Bayley F. J., Owen J. M., The Fluid Dynamic of a Shrouded Disk System With a Radial Outflow of Coolant, ASME Journal of Engineering for Power , 92: 335 (1970).
[9] Phadke U. P., Owen J. M., An Investigation of Ingress for an Air-Cooled Shrouded Rotating Disk System With Radial Clearance Seals", ASME Journal of Engineering for Gas Turbine and Power, 105: 178-182 (1983).
[10] Launder B., Poncet S,, Serre E., Laminar, Transitional and Turbulent Flows in Rotor-Stator Cavities, School of Mechanical, Aerospace & Civil Engineering, The University of Manchester (2010).
[11] Poncet S., Schiestel R., Chauve M.P., Turbulence Modelling and Measurements in a Rotor-Stator System with Throughflow, Engineering Turbulence Modelling and Experiments ETMM6, Elsevier (New-York) 761-770 (2005).
[12] Orszag S. A., Yakhot V., Flannery W. S., Boysan F., Choudhury D., Maruzewski J., Patel B., Renormalization Group Modeling and Turbulence Simulations", In International Conference on Near-Wall Turbulent Flows, Tempe, Arizona (1993).